ACS APPLIED MATERIALS & INTERFACES

Research Article

www.acsami.org

Antimony-Mediated Control of Misfit Dislocations and Strain at the Highly Lattice Mismatched GaSb/GaAs Interface

Yi Wang,[*,†] Pierre Ruterana,[*,†] Jun Chen,[†] Slawomir Kret,[‡] Salim El Kazzi,[§] Cecile Genevois,[¶] Ludovic Desplanque,[§] and Xavier Wallart[§]

[†]CIMAP, CNRS UMR 6252, 6 Boulevard du Maréchal Juin, 14050 Caen Cedex, France

[‡]Institute of Physics PAS, AL. Lotników 32/46, 02-668 Warszawa, Poland

[§]IEMN, UMR-CNRS 8520, CS 60069, 59652 Villeneuve d'Ascq Cedex, France

[¶]GPM, CNRS UMR6634, Avenue de l'université, BP 12, 76801 Saint-Etienne-du-Rouvray, France

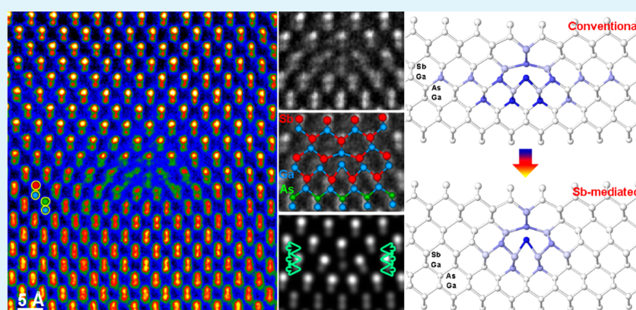

ABSTRACT: Determining the atomic structure of misfit dislocations at highly lattice mismatched interface is essential to optimize the quality of the epitaxial layer. Here, with aberration corrected scanning transmission electron microscopy at sub-Angstrom resolution and molecular dynamics simulation, we investigated the atomic structure of misfit dislocations at GaSb/GaAs interface. New types of Lomer misfit dislocation formed on an Sb wetting monolayer were observed, in contrast to a conventional misfit dislocation whose core is located at interface. These Sb-mediated dislocations have highly localized cores and offer more capability to confine the mismatch strain at the interface. The low strain atomic configuration of Sb-mediated dislocations is driven by minimization of the core energy. This unveiled mechanism may pave the way to the growth of high quality hetero-epitaxial layers.

KEYWORDS: *antimonides, misfit dislocation, lomer dislocation, aberration corrected scanning transmission electron microscopy, molecular beam epitaxy, molecular dynamics simulation*

1. INTRODUCTION

Interfacial misfit dislocations in lattice-mismatched hetero-epitaxial growth of diamond cubic and zinc blend materials, including 60° dislocation, Lomer dislocation, and 60° dislocation pair,[1,2] have been the focus of materials research for decades owing to their critical role in strain relaxation as well as in the crystal quality of the epitaxial layers.[3,4] Optimizing the crystal quality of highly lattice mismatched epitaxial layers requires a detailed understanding of the misfit dislocation structure and its role in strain relaxation of the epitaxial layer. Over the last years, there has been significant progress in the understanding of these issues, mainly because of recent advances in atomic-scale characterization techniques such as aberration-corrected transmission electron microscopy (TEM)[5,6] and strain mapping,[7] in combination with the use of atomic-scale modeling techniques.[8] Because of applications in optoelectronic and ultra-high speed low-power consumption electronics,[9−11] there is a demand for improving the epitaxy for Sb-based semiconductors. One path to this improvement is through the interface misfit (IMF) growth mode, where the lattice mismatch strain can be confined and relieved at the interface by a cross grid network of parallel Lomer dislocations lying in [110] and [$1\bar{1}0$] directions, with a spacing of 5.51 nm. The IMF growth mode leads to high quality epitaxial layers with a low density of threading dislocations ($<10^6$ cm^{-2})[12] and opens the way to the integration of Sb-(opto)electronics on GaAs (or on Si).[13,14] In this growth mode, a carefully monitoring of the substrate surface reconstruction through an exposure to Sb flux promotes the formation of Lomer dislocations at interface and appears to be critical for the epitaxial layer quality.[12−14] Although the IMF grown mode has shown in some instances to be particularly successful in reducing the dislocation densities, until now, the systematic growth reproducibility of the high quality layers has not yet been attained owing to a still poor understanding of the mechanisms involved, especially the role of Sb surface treatment which we refer in this paper to as Sb-mediated growth. Indeed, it is presumed that this mode may randomly give rise to threading dislocation densities in the range between 10^6−10^8 cm^{-2}.[15] Therefore, it is clear that more detailed work is still needed to explain the mechanisms involved, and help to improve the quality of the epitaxial layer in a reproducible way.

In this work, we report on a combined experimental and theoretical study of the atomic structure of highly lattice mismatched hetero-interfaces (GaSb/GaAs = 7.8%). Aberration-corrected high angle annular dark field (HAADF) imaging

Received: July 18, 2013
Accepted: September 11, 2013
Published: September 11, 2013

ACS Publications © 2013 American Chemical Society

was used to obtain structural and chemical information, atom by atom, at the interfaces and for the misfit dislocations. A comprehensive molecular dynamics (MD) simulation was applied to evaluate the stability of the misfit dislocations and to reveal the role of Sb on the misfit dislocations formation.

2. EXPERIMENTAL AND COMPUTATIONAL DETAILS

The samples were grown on GaAs (001) semi-insulating substrates by molecular beam epitaxy (MBE) in a 3-inch Riber Compact 21TM reactor with a base pressure better than 1×10^{-10} Torr. After the deoxidization of the GaAs substrate at 625 °C under an As flux, a 300 nm GaAs layer was first grown at 580 °C to smooth the surface. Then the Ga and As valves were closed and the sample temperature was decreased to 460 °C. At this stage, the GaAs surface exhibits a (4x6) reconstruction, monitored by in situ reflection high-energy electron diffraction (RHEED) and characteristic of a Ga rich surface. After an exposure to Sb flux, the (1 × 3) surface reconstruction of GaAs-Sb was generated as monitored by RHEED. Following the confirmation of the (1 × 3) substrate surface reconstruction, 100 MLs (monolayers) of GaSb were deposited. The growth rate was 0.7 ML/s for the GaSb layers with a Sb flux of 2.5 ML/s. Cross-sectional TEM samples were prepared by a standard procedure including grinding, dimpling, and final argon ion beam milling in a stage cooled with liquid nitrogen at −150 °C to minimize ion beam damage.

The HAADF-STEM imaging experiments were performed with a JEOL ARM200F microscope, equipped with a probe spherical aberration corrector, operating with a 0.1 nm probe at an accelerating voltage of 200 kV. The convergence semi-angle for the incident probe was 31 mrad, and the collection angle of the HAADF detector was in a range of 50−180 mrad. HAADF-STEM image simulation was performed using the QSTEM software package[16] with the atomic structure model of Lomer misfit dislocation obtained by MD simulation.

The simulated relaxation of GaSb/GaAs heterostructures was performed by MD simulation using the Stillinger−Weber potential[17] reported by Ichimura[18] and periodic boundary conditions along [110], [1$\bar{1}$0], and [001] directions. The Lomer misfit dislocation was constructed in a series of supercells of various sizes in *xy* plane ((001) plane), 26a × 26a for GaSb and 28a × 28a for GaAs (a: corresponding {110} lattice spacing of GaAs and GaSb), respectively; the supercell was made up of 30 MLs GaSb sandwiched between two 20 MLs GaAs along the *z* direction. The relaxation procedures were performed using the quench algorithm[19] and they were stopped when the system kinetic temperature was lower than 10^{-8} K. The Sb wetting was modeled by modifing relaxed supercells of the conventional misfit dislocation and carrying out a new relaxation procedure.

3. RESULTS AND DISCUSSION

In III−V cubic compounds, the dislocations are expected in {111} planes with their Burgers vectors along ⟨110⟩ directions. Two atomic structures of the Lomer dislocation in diamond structure were proposed by Hornstra,[20] and later confirmed by experimental observations.[3,21,22] The first one, namely the shuffle set, consists of structural units of five and seven atomic rings; the other structure, denoted as the glide type, consists of an eight atomic ring with an inner atom and a dangling bond. In this section, we investigate the influence of the Sb-mediated growth on these two types Lomer dislocation. As can be seen in the HAADF image of GaSb/GaAs interface observed along [1$\bar{1}$0] zone axis (Figure 1a), the GaSb and GaAs dumbbells are clearly resolved. In the epitaxial layer Sb (Z_{Sb} = 51) atom columns appear brighter than the Ga (Z_{Ga} = 31) atom columns (the contrast in HAADF images is proportional to $\sim Z^2$ in first approximation[23,24]), while in substrate region, the intensity of As (Z_{As} = 33) atom columns is only slightly higher than for the Ga atom columns, and quite similar in thicker areas. The

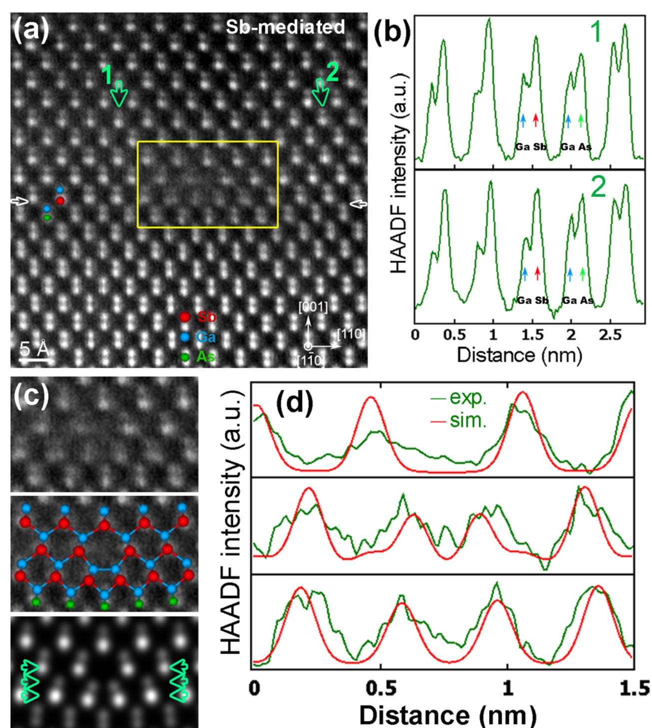

Figure 1. (a) HAADF-STEM micrograph of an Sb-mediated shuffle Lomer misfit dislocations at GaSb/GaAs interface in [1$\bar{1}$0] projection. (b) Intensity profiles obtained across the 5 dumbbells at interface indicated by the arrows. (c) The highlighted region superimposed with atomic models obtained by MD simulation, as well as simulated HAADF-STEM image of the atomic model. (d) Intensity profiles across the dislocation core region indicated by the arrows in image c.

position of the interface can be detected by examining the HAADF image intensity. Figure 1b shows image intensity profiles obtained across the interface region as indicated by the arrows. In these profiles, the Sb, Ga, and As atomic columns at interface are clearly identified by comparing the image intensity peaks of each dumbbell, and the atomic species of the columns at the interface have been labeled in Figure 1a and b. Looking at the misfit dislocation in the figure, it has two {111} additional planes and the core structure consists of five- and seven- atom cycles indicating a shuffle set configuration.[20] However, considering the position of the dislocation core in reference to the interface, it is different from the conventional shuffle set Lomer dislocation[21,22] where the five- and seven- atom rings are located below and above the interface, respectively. An example of a conventional shuffle set Lomer dislocation, which is observed in samples where the initial growth was not Sb-mediated, is presented for comparison in Figure 2. In the case of Sb-mediated shuffle set Lomer dislocation, the five- and seven-atom rings are both located above the interface. This feature indicates that the corresponding Lomer dislocation has been generated on top of an Sb wetting layer. A magnified view of the dislocation core area enclosed by the yellow square in Figure 1a is exhibited in Figure 1c together with the structural model obtained by MD simulation. The simulated HAADF image of this structural model using the multislice method (QSTEM software package)[16] is also shown in Figure 1c. As can be seen in the line profiles (Figure 1d) acquired across the dislocation cores as indicated by the arrows in Figure 1c, there is a good agreement between the simulated and the experimental HAADF images.

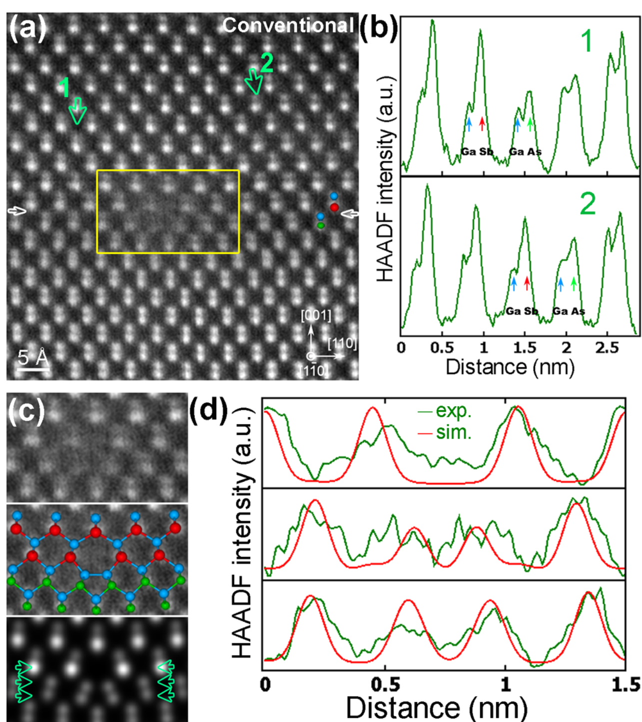

Figure 2. (a) HAADF image of a conventional shuffle set Lomer dislocation whose five and seven atomic rings are located below and above the interface, respectively. (b) Intensity profile across the interface clearly indicating the position of the GaSb/GaAs interface. (c) Highlighted region superimposed with atomic models obtained by MD simulation, as well as simulated HAADF-STEM image of the atomic model. (d) Intensity profiles across the dislocation core region indicated by the arrows in image c.

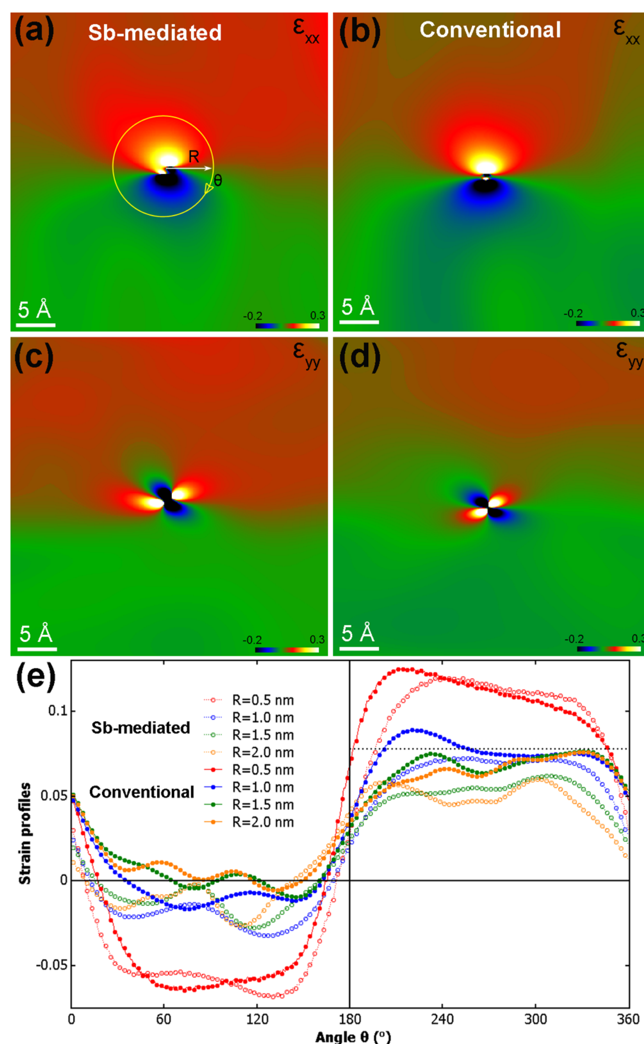

Figure 3. (a–d) Strain components ε_{xx} and ε_{yy} obtained by geometric phase analysis from Figures 1a and 2a, respectively. (e) Comparison of the strain profiles acquired around the dislocations as schematically shown in panel a by overlaid circles with radii of 0.5 (red), 1 (blue), 1.5 (green), and 2 nm (orange). The black dotted line indicating the lattice mismatch (7.8%) of GaSb/GaAs.

A comparison of capability of conventional and Sb-mediated misfit dislocation in strain relaxation (or confining the mismatch strain at interface) has been carried out by Geometric phase analysis (GPA)[7,25] of the HAADF images. Figure 3 shows the strain components ε_{xx} and ε_{yy} obtained by GPA from Figure 1a and 2a. As can be seen from both ε_{xx} and ε_{yy} in Figure 3, the misfit strain is more completely relieved by Sb-mediated Lomer dislocations in contrast to the case of the conventional Lomer dislocations. A detailed comparison of strain relaxation in the vicinity of the two dislocation types is shown in Figure 3e. In Figure 3e, the range of angles less than and greater than 180 degrees correspond the strain field of the substrate and the epitaxial layer, respectively. It is worth noticing that the dislocation core region (R = 0.5 nm) is highly strained both in substrate and epitaxial layer. With increasing radius (R), the ε_{xx} of the Sb-mediated Lomer dislocation are closer to zero in substrate and to 7.8% in epitaxial layer, respectively, in contrast to the conventional Lomer dislocation. This indicates that the Sb-mediated Lomer dislocation has more capability to confine the mismatch strain at the interface. This is also visible in ε_{yy} strain component where the transition between the substrate and epitaxial layer in Figure 3c is shaper than that in Figure 3d.

When the observations are carried out along [110] zone axis, the interface exhibits the glide set of Lomer dislocations[20] with six and eight atom rings (Figure 4a). Again, looking at the position of GaSb/GaAs interface (Figure 4b, a comparison of the experimental and simulated HAADF image can be found in Figure 4c and d), one notices that the six and eight atom rings of the dislocation core are located above the interface, indicating that the Sb wetting layer is contiguous throughout the surface upon which it was initially deposited.

To gain insight into the origin of these changes of dislocation position as related to the interface, we investigated the stability of these misfit dislocations by MD simulation. Four stable configurations are shown in Figure 5: two of which (S.C. and G.C.) are conventional ones in which the dislocation core is located exactly at interface, and in Figure 5c and d, where they have been modified so that the cores are located one monolayer above the interface. We then determine as usual, the core energy of the dislocations, by calculating the energy per unit length of dislocation, inside a cylinder of radius R (in Figure 5, the dislocation is in a cylinder of 2 nm radius), as $E(R) = ((G|b|)^2/(4\pi(1-\nu)))\ln(R/R_c) + E_c$, $(R \geq R_c)$, where G is the shear modulus, ν is the Poisson's ratio, b is the Burgers vector, R_c is the core radius, and E_c is the core energy per unit length.[26] Figure 6 shows the $E(R)$ curves for these Lomer dislocations. Apparently, the dislocations with one monolayer Sb wetting layer have lower core energy and smaller core radii in comparison to the conventional ones. The calculated core

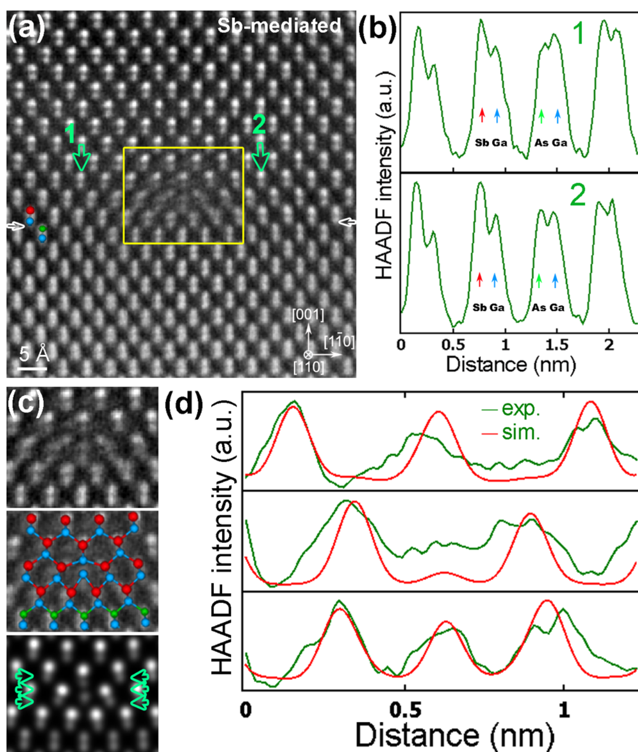

Figure 4. (a) HAADF-STEM image of an Sb-mediated glide set Lomer misfit dislocations at the GaSb/GaAs interface along the [110] projection. (b) HAADF intensity profiles obtained across the 4 dumbbells at interface indicated by the arrows. (c) Highlighted region superimposed with atomic models, as well as simulated HAADF-STEM image of the atomic model. (d) Intensity profiles across the dislocation core region indicated by the arrows in image c.

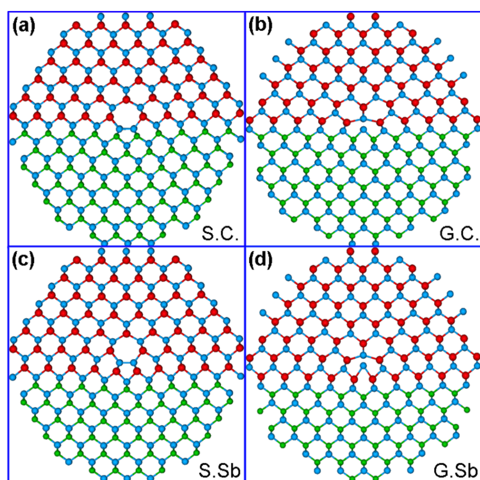

Figure 5. Relaxed atomic structures of the shuffle [S.C. and S.Sb in panels a and c] and glide [G.C. and G.Sb in panels b and d] set Lomer dislocations cores in a cylinder of 2 nm radius. Red, green, and blue spheres represent Sb, As, and Ga atoms, respectively; S.C. and G.C. are the conventional configurations (without Sb wetting), and S.Sb and G.Sb are the modified configuration by 1 ML Sb wetting.

energy (E_c), core radii (R_c), and shear modulus (G) of the Lomer dislocations are summarized in Table 1. As can be noticed, the shear modulus values are between those of GaSb (24.1 GPa) and GaAs (32.5 GPa)[27] meaning that this procedure can reasonably account for interfacial phenomena. Therefore, the configurations with the core located above the

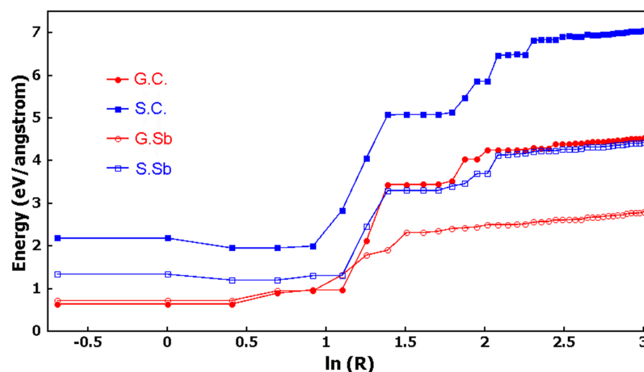

Figure 6. Energy per unit length (eV/Å), $E(R)$ for the different Lomer dislocations plotted as a function of distance from the dislocation core center. The energy is evaluated for a cylinder of radius R around the dislocation core.

Table 1. Calculated Core Energy (E_c), Core Radii (R_c), and Shear Modulus (G) of the Lomer Dislocations

	S.C.	G.C.	S.Sb	G.Sb
R_c (Å)	10	7.5	8	4.5
E_c (eV/Å)	6.83	4.25	4.14	2.32
G (GPa)	29.54	28.25	28.09	28.18

interface are more stable than the conventional ones with the core at the interface. In contrast to moving the dislocation core into the GaSb, when we carried out the simulations after moving the dislocation core into the substrate, it has not been possible to complete the relaxation process (the system kinetic temperature cannot reach 10^{-8} K), indicating that such configurations are not stable.

Figure 7 shows the energetically colored map of the Glide set Lomer misfit dislocation (configurations G.C. and G.Sb for instance). In this figure, a white-blue color palette has been applied to emphasize the changes in energy following the corresponding color bar. Atoms of the lowest and the highest energy are given in white and blue color, respectively. As can be seen in Figure 7a, along the vertical direction, the energy decreases rapidly; however, along the interface the energy distribution is more extended. Moreover, as could be expected, the atoms of high energy are located at the interface, namely Ga, and each forms two bonds with Sb and two bonds with As. Shifting this Lomer dislocation core into GaSb by Sb wetting leads to an energetically more localized core as shown in Figure 7b.

To understand the mechanism underlying the decrease in core energy in Figure 6, we have analyzed the bond lengths along the interface at the dislocation core region. Taking configuration G.C. and G.Sb as an example, the curves in Figure 7c show the deformation of the bonds with reference to the bulk materials ($\varepsilon = (l - l_{bulk})/l_{bulk}$, where l is the measured bond length and l_{bulk} is the bond length of the bulk material) as a function of the distance to the dislocation core. The labels represent the different bonds as indicated in Figure 7a and b where configurations G.C. and G.Sb are shown in red and blue, respectively. In configuration G.C., the g bonds are in compression and the c and the h bonds are in tension; whereas in configuration G.Sb, all the c, g, and h bonds are in compression and the magnitude of the deformation is smaller. Therefore, moving the dislocation core up one monolayer into GaSb compensates for the bending of the interfacial atomic

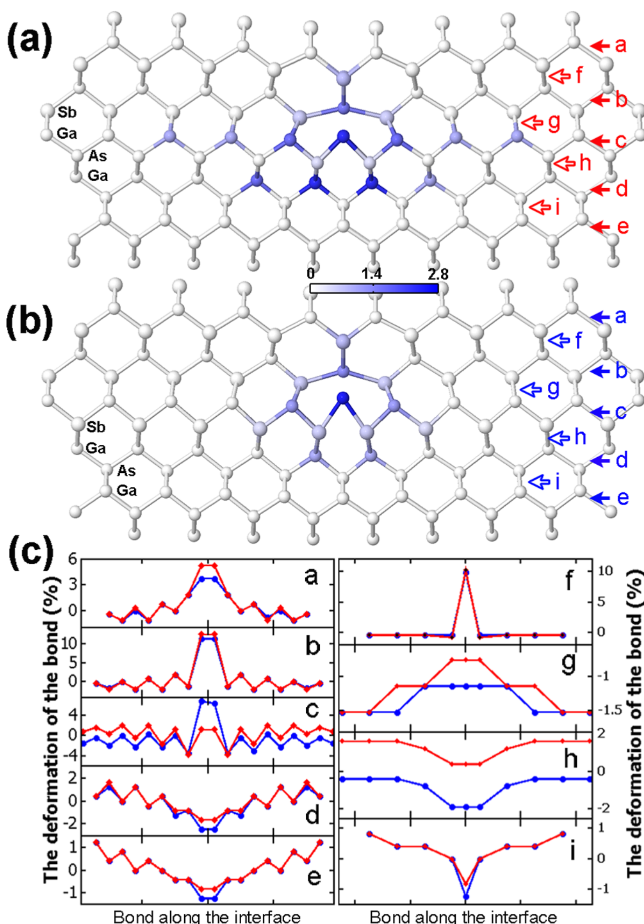

Figure 7. (a and b) Energy distribution in configurations G.C. and G.Sb, the interface of GaSb/GaAs have been labeled. The color intensity of the atoms reflects their energy, the reference energy corresponds to the lowest (white) and highest (blue) energy, the unit of the scale bar is eV. (c) Deformation of the bond in configurations G.C. and G.Sb at the dislocation core, the label of the curves indicates the different bonds, see arrows and letters in panels a and b. The deformation was defined as $\varepsilon = (l - l_{bulk})/l_{bulk}$, where l is the bond length and l_{bulk} is the bond length of the bulk material.

bonds. We also carried out the same detailed analysis on the shuffle set misfit dislocations and the results led to the same conclusion.

4. CONCLUSION

In this work, we report on the impact of Sb wetting on the atomic configuration of misfit dislocations at the highly lattice mismatched GaSb/GaAs interface. This sub-angstrom resolution HAADF analysis of the interface and the misfit dislocations shows that the Sb wetting (substrate surface preparation) leads to change in the atomic configuration of the interface dislocations: the new Lomer dislocations' core is located above the GaSb/GaAs interface, in contrast to a conventional one whose core is located at interface. These new types of dislocations have highly localized cores and offer more capability to confine the mismatch strain at the interface. The comprehensive MD simulation shows that the change in their atomic configuration is driven by minimization of the core energy. Of importance in this finding is that this mechanism underlines the role of the initial growth conditions on the misfit dislocations array and it may suggest strategies for the production of low defect density epitaxial layers in high mismatch cubic materials of critical technological applications.

AUTHOR INFORMATION

Corresponding Authors

*E-mail: yi.wang@ensicaen.fr.

*E-mail: pierre.ruterana@ensicaen.fr.

Notes

The authors declare no competing financial interest.

ACKNOWLEDGMENTS

This work was supported by the National Research Agency under project MOS35, Contract No. ANR-08-NANO-022.

REFERENCES

(1) Narayan, J.; Oktyabrsky, S. *J. Appl. Phys.* **2002**, *92*, 7122−7127.

(2) Wang, Y.; Ruterana, P.; Kret, S.; El Kazzi, S.; Desplanque, L.; Wallart, X. *Appl. Phys. Lett.* **2013**, *102*, No. 052102.

(3) Vilà, A.; Cornet, A.; Morant, J.R.; Loubradou, M.; Bonnet, R.; Gonzalez, Y.; Gonzalez, L.; Ruterana, P. *Philos. Mag. A* **1995**, *71*, 85−103.

(4) Qian, W.; Skowronski, M.; Kaspi, R.; De Graef, M.; Dravid, V. P. *J. Appl. Phys.* **1997**, *81*, 7268−7272.

(5) Urban, K. W. *Science* **2008**, *321*, 506−510.

(6) Krivanek, O.L.; Chisholm, M.F.; Nicolosi, V.; Pennycook, T.J.; Corbin, G.J.; Dellby, N.; Murfitt, M.F.; Own, C.S.; Szilagyi, Z.S.; Oxley, M.P.; et al. *Nature* **2010**, *464*, 571−574.

(7) Hÿtch, M.J.; Putaux, J.L.; Pénisson, J.M. *Nature* **2003**, *423*, 270−273.

(8) Sinnott, S.B.; Brenner, D.W. *MRS Bull.* **2012**, *37*, 469−473.

(9) Bennett, B.R.; Magno, R.; Boos, J.B.; Kruppa, W.; Ancona, M.G. *Solid-State Electron.* **2005**, *49*, 1875−1895.

(10) del. Alamo, J.A. *Nature* **2011**, *479*, 317−323.

(11) Baxter, J. *Nat. Photonics* **2012**, *6*, 212.

(12) Huang, S.; Balakrishnan, G.; Huffaker, D. L. *J. Appl. Phys.* **2009**, *105*, No. 103104.

(13) Huang, S.H.; Balakrishnan, G.; Khoshakhlagh, A.; Jallipalli, A.; Dawson, L.R.; Huffaker, D.L. *Appl. Phys. Lett.* **2006**, *88*, No. 131911.

(14) El Kazzi, S.; Desplanque, L.; Coinon, C.; Wang, Y.; Ruterana, P.; Wallart, X. *Appl. Phys. Lett.* **2010**, *97*, No. 192111.

(15) Hopkins, P.E.; Duda, J.C.; Clark, S.P.; Hains, C.P.; Rotter, T.J.; Phinney, L.M.; Balakrishnan, G. *Appl. Phys. Lett.* **2011**, *98*, No. 161913.

(16) Koch, C.T. *Determination of Core Structure Periodicity and Point Defect Density along Dislocations*; Arizona State University: Phoenix, AZ, 2002.

(17) Stillinger, F.H.; Weber, T.A. *Phys. Rev. B: Condens. Matter Mater. Phys.* **1985**, *31*, 5262−5271.

(18) Ichimura, M. *Phys. Status Solidi A* **1996**, *153*, 431−437.

(19) Verlet, L. *Phys. Rev.* **1967**, *159*, 98−103.

(20) Hornstra, J. *J. Phys. Chem. Solids* **1958**, *5*, 129−141.

(21) McGibbon, A.J.; Pennycook, S.J.; Angelo, J.E. *Science* **1995**, *269*, 519−521.

(22) Lopatin, S.; Pennycook, S.J.; Narayan, J.; Duscher, G. *Appl. Phys. Lett.* **2002**, *81*, 2728−2730.

(23) Pennycook, S.J.; Jesson, D.E. *Ultramicroscopy* **1991**, *37*, 14−38.

(24) Carlino, E.; Grillo, V. *Phys. Rev. B: Condens. Matter Mater. Phys.* **2005**, *71*, 235303.

(25) Hÿtch, M. J.; Snoeck, E.; Kilaas, R. *Ultramicroscopy* **1998**, *74*, 131−146.

(26) Hirth, J. P.; Lothe, J. *Theory of Dislocations*, 2nd ed.; Wiley-Interscience: New York, 1982; p 59−95.

(27) S. Adachi, *Properties of Group-IV, III−V and II−VI Semiconductors*; Wiley-Interscience: Chichester, U.K., 2005; p 58.